

Title Transponders for millimeter wave  
identification  
Author(s) Pursula, Pekka; Donzelli, Francesco  
Citation IEEE APS Topical Conference on  
Antennas and Propagation in  
Wireless Communications, APWC,  
Torino, Italy, 12-16 September 2011,  
pp. 1221-1224  
Date 2011  
Rights Copyright © (2011) IEEE.  
Reprinted from IEEE APS Topical  
Conference on Antennas and  
Propagation in Wireless  
Communications, APWC.  
This article may be downloaded for  
personal use only

VTT  
<http://www.vtt.fi>  
P.O. box 1000  
FI-02044 VTT  
Finland

By using VTT Digital Open Access Repository you are bound by the following Terms & Conditions.

I have read and I understand the following statement:

This document is protected by copyright and other intellectual property rights, and duplication or sale of all or part of any of this document is not permitted, except duplication for research use or educational purposes in electronic or print form. You must obtain permission for any other use. Electronic or print copies may not be offered for sale.

# Transponders for Millimeter Wave Identification

Pekka Pursula<sup>1</sup> and Francesco Donzelli<sup>2</sup>

**Abstract** — Radio frequency identification at millimeter waves enables new applications, such as high data rate short range communication, location sensing through narrow-beam antennas etc. In this paper two transponders designs for 60 GHz Millimeter wave identification (MMID) system are presented. One transponder consists of a Schottky diode and an antenna on LCP and the other of a backward tunneling diode and an antenna on LTCC. The design, fabrication and measurements of the two designs are presented, and compared to simulations and each other.

**Index Terms** — Video detector, Radio Frequency Identification, RFID, millimeter waves, millimeter wave identification, MMID.

## I. INTRODUCTION

Ultra High Frequency Radio frequency identification (UHF RFID) has spread throughout the industry especially in logistics applications. UHF RFID system consists of a reader and passive, i.e. batteryless transponders, or tags, which communicate to the reader by backscattering modulation.

Millimeter Wave Identification (MMID) updates the RFID system to millimeter waves [1]. The higher carrier frequency has several advantages: First, smaller antennas enable miniaturized transponders as well as compact reader modules. Second, antenna arrays can be used to achieve narrow beam reader antennas, which enable efficient transponder localization. Third, relaxed radio regulations at 60 GHz enable high data rate communication.

Downlink communication in an MMID system is based on amplitude modulation that is received by a diode detector in the tag. Uplink communication is based on backscattering modulation. Many semipassive, i.e. battery-assisted, transponders have been reported in the literature, e.g. [2], [3], but also passive transponders have been demonstrated at millimeter waves [4], [5]. The readers can be miniaturized using advanced packaging technologies, such as LTCC [6], or automotive radars can be utilized as the reader devices [7].

A semipassive MMID transponder (Fig. 1) consists of an antenna array, matching circuit, a diode and a bias network. Low pass filter at each terminal ensures the millimeter wave signal to be cut off from the baseband. In addition to detection, the diode is can used as a modulator: The diode bias is modulated to achieve two different antenna load (or reflection) states, hence modulating the antenna scattering.

The power received and the power scattered can be described by the effective aperture  $A_e$  and the radar cross section  $\sigma_m$  of the transponder, respectively [1]:

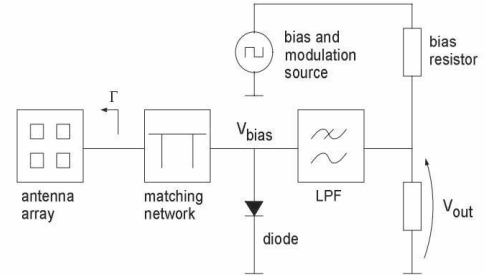


Fig. 1. Block diagram of a semipassive MMID transponder.

$$A_e = \beta \frac{G_A \lambda^2}{4\pi} (1 - |\Gamma_0|^2) \quad (1)$$

$$\sigma_m = \frac{G_A^2 \lambda^2}{16\pi} |\Gamma_1 - \Gamma_2|^2, \quad (2)$$

where  $G_A$  is the transponder antenna gain. The reflection coefficient  $\Gamma_0$  presents detection, and  $\Gamma_1$  and  $\Gamma_2$  modulation bias states.

The detected voltage  $V_{out}$  of the transponder can be calculated from (1) with the diode sensitivity  $\beta$  and Friis equation. Similarly, the power received by the reader can be calculated from (2) and the radar equation.

This paper presents the design two MMID transponders: One built on low temperature co-fired ceramic (LTCC) with a backward diode, and another built on liquid crystal polymer (LCP) with a Schottky diode. The LTCC transponder represents a high-end solution with a backward diode on an expensive but high-performance substrate. On the contrary, the LCP transponder utilizes low-price substrate that can be patterned with standard PCB process, on which a typical millimeter wave Schottky diode is placed.

## II. DESIGN AND FABRICATION

### A. Diodes

The backward diode manufactured by HRL provides zero bias detection with high sensitivity (up to  $\beta = 15\,000$  mV/mW) [10]. The I-V curve of the diode (Fig. 2) is described as a polynomial model (including nonlinear capacitance) for simulation purposes. The diode is supplied as bare die for flip chip connection.

<sup>1</sup> VTT Technical Research Centre Finland, P.O.Box 1000, FI-02044, Espoo, Finland, email pekka.pursula@vtt.fi.

<sup>2</sup> DEIS, University of Bologna, Bologna, Italy, email Francesco.donzelli@unibo.it.

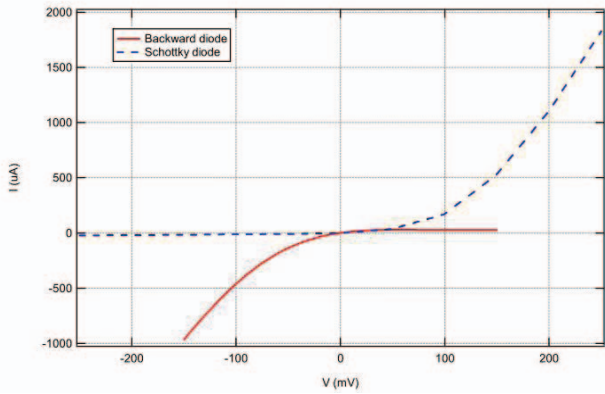


Fig. 2. Measured I-V curve of the backward diode and the Schottky diode.

The Schottky diode (Agilent GaAs HSCH-9162) is available in a beam-lead package to facilitate a reflow-type diode attachment. A sensitivity of  $\beta = 500$  mV/mW is provided [11] with low forward bias (1-100 $\mu$ A). For non-linear modelling we used an anti-parallel diode pair configuration, whose electrical specifications are series resistance  $R_{S1} = 50 \Omega$ , saturation current  $I_{S1} = 12 \mu\text{A}$ , zero-bias junction capacitance  $C_{j01} = 0.03$  pF and ideality factor  $n_1 = 1.2$  for the forward device and  $R_{S2} = 10 \Omega$ ,  $I_{S2} = 84 \mu\text{A}$ ,  $C_{j02} = 0.03$  pF and  $n_2 = 40$  for the reverse one.

### B. LTCC transponder

The LTCC transponder (Fig. 3) takes advantage of the multilayer properties of the LTCC technology. The aperture coupled 2x2 antenna array uses four layers of Ferro A6-S LTCC material ( $h = 96 \mu\text{m}$  per layer, 4 layers used,  $\epsilon_r = 5.74$ ,  $\tan\delta = 0.0023$ ) [12]. Wilkinson power dividers were used in the binary feed network. The antenna arrays are similar to the one shown in Fig. 5 in [9] but 4 array elements were used instead of 16. The simulated -10-dB frequency band is 58.8–62.6 GHz and gain 11.1 dBi at 61 GHz.

The design of the matching circuit has two objectives: For sensitive reception, the best possible match to the diode is needed. For backscattering modulation, two diode bias states with the greatest difference in reflection coefficient is required. Stub matching is used between diode and antenna, and low-pass filter is implemented with a radial stub.

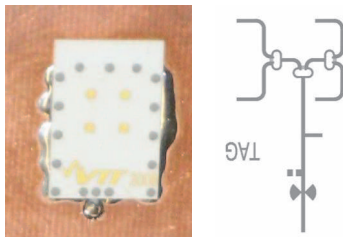


Fig. 3. LTCC transponder: Photograph of the antenna side (left) and schematic of the feed network (right).

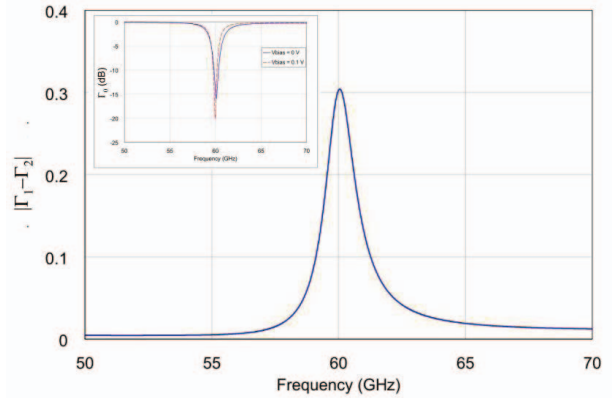


Fig. 4. LTCC transponder: Modulated reflection coefficient  $|\Gamma_1 - \Gamma_2|$ . Inset: Matching of the impedance states  $\Gamma_1$  and  $\Gamma_2$ .

The HRL diode is used in the LTCC transponder with low bias voltages: zero bias for detection and 0 V – 0.1 V for modulation. Simulation results of matching and difference in  $|\Gamma_1 - \Gamma_2|$  are presented Fig. 4.

### C. LCP Transponder

The LCP transponder (Fig. 5.) was designed for low-cost fabrication with LCP substrate Rogers UltraLam3850 ( $h = 100 \mu\text{m}$ , Cu thickness = 5  $\mu\text{m}$ ,  $\epsilon_r = 2.9$ ,  $\tan\delta = 0.0025$ ) [13]. Only the top copper layer is patterned, including the radiating antenna elements, the antenna feed network, and matching network. The feed network used reactive power splitters to avoid resistors in the Wilkinson design [8]. The serial feed network keeps the radiating elements in phase at 60 GHz with patch size of  $W = 2$  mm,  $L = 1.43$  mm and inter-patch separation of  $L_s = 2.43$  mm. Simulated directivity of 18 dB is achieved with an impedance bandwidth of 1 GHz (-10dB).

The diode is placed in parallel between a 60 GHz matching section towards the antenna side and two radial-stub-based low pass filters positioned on both cathode and anode. A further radial stub inserted near the anode provides a RF ground, thus avoiding via-holes on LCP fabrication process.

The Schottky diode bias levels are 0 V and 0.5 V. Simulation results of matching and difference in  $|\Gamma_1 - \Gamma_2|$  are presented Fig. 6. Between 60 and 62 GHz a good matching is achieved at 0 V while the shift between the two impedance levels looks promising for uplink modulation.

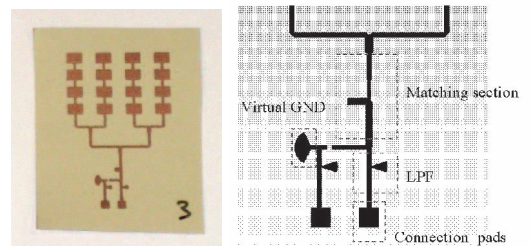


Fig. 5. LCP transponder: Photograph (left) and schematic of the feed network (right).

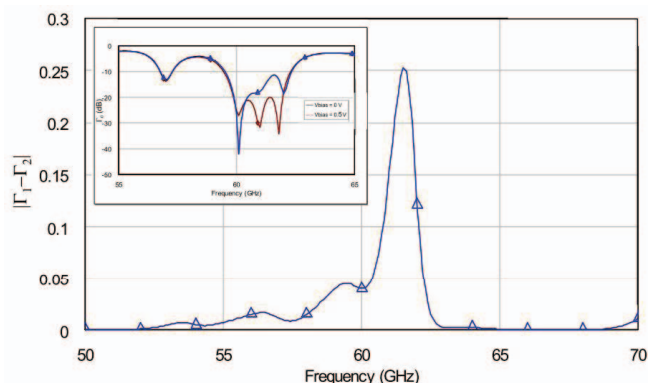


Fig. 6. LCP transponder: Modulated reflection coefficient  $|\Gamma_1 - \Gamma_2|$ . Inset: Matching of the impedance states  $\Gamma_1$  and  $\Gamma_2$ .

#### IV. MEASUREMENTS

For experimental verification, a waveguide-based reader device of Fig. 7 was assembled (see Fig. 1 for transponder schematic). The quadrupler (OML S15MS-AG) provided 3 - 4 dBm power for the 24-dB TX horn antenna. Receiver consisted of a mixer-amplifier (Spacek PV-VB) and a spectrum analyzer (Agilent E4407B). The LO frequencies are chosen so that the IF frequency is 100 MHz.

The output voltage of the diode was measured with a high-impedance digital voltmeter to characterize the diode as a receiver. Friis equation and Eq. (1) with the simulated transponder antenna gain was used for calculating the power incident to the diode. Received modulated backscattering power was measured with the spectrum analyzer, while the tag diode bias was modulated. Modulated reflection coefficient was calculated with radar equation and (2). The LTCC tag was measured at a distance of 20 cm and LCP tag at 60 cm. Backscattered spectra of the LCP transponder can be seen in Fig. 8.

The modulated sensitivities and reflection coefficients are presented in Figs. 9 for the LCP tag. The LTCC tag presents only sensitivity (Fig. 10) due to problems in power calibration of the backscattering measurement.

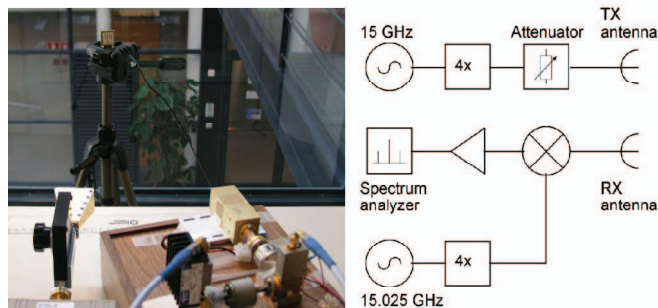


Fig. 7. Measurement setup: Photograph of the reader and the tag (left) and schematic of the reader (right).

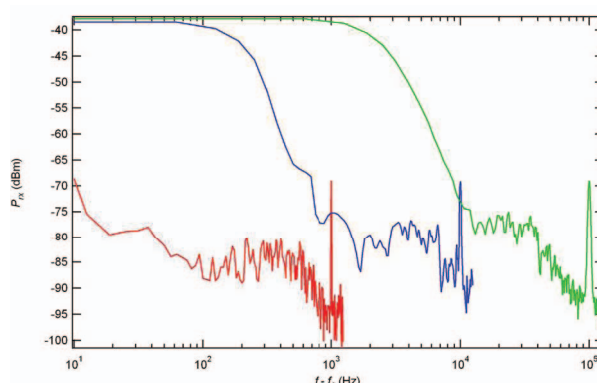


Fig. 8. LCP transponder: Received scattered spectra with different modulation frequencies.

The sensitivities and the modulated reflection coefficients are an order of magnitude lower than expected from simulations. However, the results especially in Fig. 9 show a good agreement in the frequency behavior between downlink and uplink measurements. Also the HRL diode is measured to be the more sensitive device, as expected from the datasheets. High input power due to low operation distance probably saturates the diode affecting the matching. Hence the sensitivity and modulated reflection coefficient is deteriorated.

Fig. 8. shows a 20-dB signal-to-noise ratio with 10 Hz, 300 Hz and 3 kHz resolution bandwidths for 1 kHz, 10 kHz and 100 kHz modulations, respectively. Hence a better modulator, e.g. a MEMS switch would allow for a very wideband short range communications.

#### V. CONCLUSION

This paper presented design and measurements of two semipassive MMID transponders at 60 GHz: Backward diode on LTCC and Schottky diode on LCP.

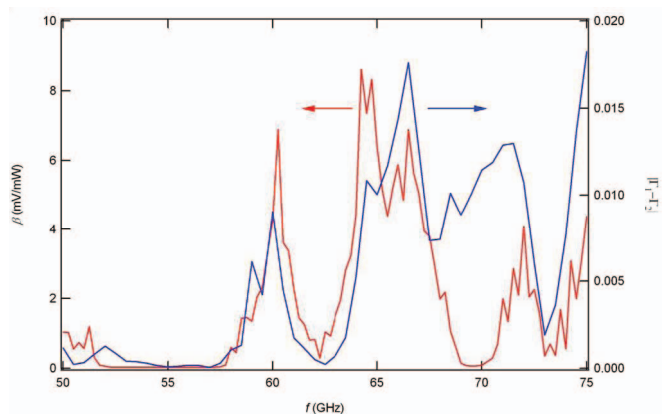


Fig. 9. LCP: Transponder: Measured sensitivity and modulated reflection coefficient.

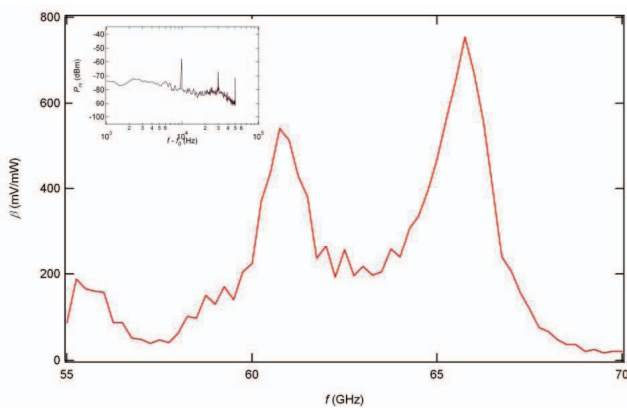


Fig. 10. LTCC transponder: Measured sensitivity. Inset: Received scattered spectrum.

The LTCC antenna provides wider bandwidth, because the multilayer capability of the LTCC process allows higher patch-ground separation. The main difference in the technologies is the price and complexity – LTCC is more expensive, and maybe even too fancy for the simple application. The LCP version is less expensive (even as low as 0.10 € [8]) and simpler to manufacture with standard PCB process. A more detailed comparison of a LTCC and LCP for 60 GHz antenna solutions can be found in [14].

The backward diode provides better sensitivity according to data sheets and measurements. In addition to this, the backward diode facilitates zero-bias detection for reduced power consumption in the tag. As modulators, the diodes perform equally well. The diodes are about as expensive in large amounts.

#### ACKNOWLEDGMENTS

The authors like to thank J. Schulman from HRL Laboratories for diode samples as well as fruitful discussion. A. Lamminen is acknowledged for the LTCC antenna design. I. Marttila, H. Hakojärvi, and M. Kantanen for help in measurements.

#### REFERENCES

- [1] P. Pursula, T. Vähä-Heikkilä, A. Müller, D. Neculoiu, G. Konstantinidis, A. Oja, J. Tuovinen, Millimetre Wave Identification — new radio system for low power, high data rate and short range, *IEEE Transactions on Microwave theory and techniques*, vol. 56, no. 10, pp. 2221-2228, Oct. 2008.
- [2] A. Müller, D. Necaliou, P. Pursula, T. Vähä-Heikkilä, F. Giacomucci, J. Tuovinen, “Hybrid integrated micromachined receiver for 77 GHz millimeter wave identification systems”, *the 37th European Microwave Conference*, Munich, Germany, Oct. 2007, pp. 1034-1037.
- [3] P. Pursula, V. Viikari, “Novel Automotive Radar Applications”, *Millimetre Wave Days (parallel conferences of The 6th ESA Workshop on Millimetre-Wave Technology and Applications, and The 4th Global Symposium on Millimeter Waves)*, Espoo, Finland, May 23-25, 2011.
- [4] S. Pellerano, J. Alvarado, Y. Palaskas, “A mm-wave power harvesting RFID tag in 90 nm CMOS,” *Custom Integr. Circuits Conf.*, San Jose, CA, Sep. 2009, pp. 677–680.
- [5] P. Pursula, F. Donzelli, H. Seppä, “Passive RFID at Millimeter Waves”, accepted in *IEEE Transactions on Microwave Theory and Techniques*, March 2011.
- [6] P. Pursula, T. Karttaavi, M. Kantanen, A. Lamminen, J. Holmberg, M. Lahdes, I. Marttila, M. Lahti, A. Luukanen, T. Vähä-Heikkilä, “60 GHz Millimeter Wave Identification Reader on 90 nm CMOS and LTCC”, *IEEE Transactions on Microwave Theory and Techniques*, vol.59, no. 4, pp. 1166 - 1173, April 2011.
- [7] V. Viikari, J. Saebboe, S. Cheng, M. Kantanen, M. Al-Nuaimi, T. Varpula, A. Lamminen, P. Hallbjörner, A. Alastalo, T. Mattila, H. Seppä, P. Pursula, A. Rydberg, “Technical Solutions for Automotive Intermodulation Radar for Detecting Vulnerable Road Users,” *IEEE 69th Vehicular Technology Conference Spring (VTC2009-Spring)*, 26-29 April 2009, Barcelona, Spain.
- [8] S. Cheng, P. Hallbjörner, A. Rydberg, “Array Antenna for body-worn automotive harmonic radar”, *Proc. of the 3<sup>rd</sup> European Conference on Antennas and Propagation (EuCAP)*, Berlin, Germany, Mar. 2009, pp. 2823-2827.
- [9] A. E. I. Lamminen, J. Säily, and A. R. Vimpari, “60-GHz patch antennas and arrays on LTCC with embedded-cavity substrates,” *IEEE Trans. Antennas Propag.*, vol. 56, no. 9, pp. 2865–2874, Sep. 2008.
- [10] J. N. Schulman, D. H. Chow, "Sb-heterostructure interband backward diodes," *IEEE Electron Device Letters*, vol.21, no.7, pp.353-355, Jul 2000.
- [11] “HSCH-9161, HSCH-9162 GaAs Detector Diode Data Sheet”, Agilent Technologies, 2007. Online, available at [www.agilent.com](http://www.agilent.com).
- [12] T. Vähä-Heikkilä, M. Lahti, “LTCC Platform for Millimeter Wave Modules”, *Millimetre Wave Days (parallel conferences of The 6th ESA Workshop on Millimetre-Wave Technology and Applications, and The 4th Global Symposium on Millimeter Waves)*, Espoo, Finland, May 23-25, 2011.
- [13] “ULTRALAM 3000 Liquid Crystalline Polymer Circuit Material Data Sheet”, Rogers Corporation, 2011. Online, available at [www.rogerscorp.com](http://www.rogerscorp.com).
- [14] S. Dumanli, D. L. Paul, C. J. Railton, "LTCC or LCP, A comparison using cavity backed slot antennas with pin curtains at 60 GHz," *Proc. of the 4<sup>th</sup> European Conference on Antennas and Propagation (EuCAP)*, Barcelona, Spain, Apr. 2010, pp.1-5.